Vacuum 131 (2016) 181–187

Contents lists available at ScienceDirect

Vacuum

journal homepage: www.elsevier.com/locate/vacuum

Multi-scale characterization of stray grain in the platform of nickel-base single crystal turbine blade

Yafeng Li, Lin Liu*, Taiwen Huang, Haifeng Wang, Jun Zhang, Hengzhi Fu

State Key Laboratory of Solidification Processing, Northwestern Polytechnical University, Shaanxi, Xi'an 710072, PR China

A R T I C L E I N F O

Article history:
Received 20 April 2016
Received in revised form
18 June 2016
Accepted 21 June 2016
Available online 22 June 2016

Keywords:
Nickel-base superalloy
Directional solidification
Stray grain
Characterization

A B S T R A C T

Through comparatively characterizing the platforms with and without stray grain in multi-scale levels, it is determined that stray grain (SG) originates from heterogeneous nucleation with randomly distributed orientations with respect to the matrix grain. This independently nucleated deleterious grain constitutes distinct macro, dendritic and γ' morphologies and forms a high angle boundary (HAB) in the conjunction area of SG and the matrix grain. Compositional distribution reveals that severe segregation could be identified in GB area due to compositional enrichment and deprivation during the last stage of solidification.

1. Introduction

Single crystals (SXs) are routinely produced in aerospace industry to manufacture turbine blades, capable of enduring the harsh service conditions to maximize the component life [1,2]. To further draw power from turbine section, blade geometry is optimized through redesigning inner cooling passages for an enhanced cooling efficiency; refractory-elements-revised alloys with higher melting points are used to withstand the incremental turbine inlet temperature; and thermal barrier coating was deposited onto SX blade surface to bear harsh oxidation and hot-corrosion environments [3,4]. Unfortunately, these improvements lead to solidification defects occur readily, such as freckle chains [5,6], low angle boundaries (LABs) [7], and SGs.

SG as the most detrimental casting defect constitutes high angle boundary (HAB) with primary grain (PG), serving as crack-initiation site to degrade mechanical properties in service. This kind of deleterious grains usually formed around re-entrant sections, like shrouds and platforms, is resulted from locally changed solidification conditions related to the changes of cross-section. Meyer et al. [8] first depicted that SG nucleated in a thermally undercooled zone caused by macroscopically curved liquidus isotherm in the platform ends. Based on several assumptions, Bussac et al. [9] derived a theoretical model to predict the SG formation. Yang [10] applied a combined cellular automaton-finite difference (CA-FD) model to simulate the effect of withdrawal rates and isothermal inclination angles on SG formation. Ma et al. [11] designed a set of experiments to measure undercoolabilities of superalloys in ceramic mold to predicate the proneness of SG formation in different alloying system. Zhang et al. [12] experimentally verified the effect of alloys' compositions on SG formation through solidifying sets of ingeniously designed castings featuring multi-platforms of different lengths. Meng et al. [13] paid attention to the effect of platform dimension on SG formation as the size of industry gas turbine blades are comparatively large than aero turbine blades, which are readily to suffer SG defect. Based on the theoretical and experimental analyses of the mechanism of SG formation, several controlling means have been proposed over the past few decades, such as variation of withdrawal rate [8], heat conductor technique [14] and grain continuators technique [8,15]. Some of those methods have already been applied to industrial production.

Although a lot of efforts have been paid to investigate the mechanism, the influencing factors of SG formation and its controlling methods, they were all based on a presumable fact that SG forms from a heterogeneous nucleation process. This has ever been verified, however, since the fact that in-situ observation of such high melting point alloy is technically impossible. Additionally, in-situ observation of lower melting point Sn–Bi alloy revealed that fragmented arms also could be a source of SG [16]. Aveson et al. [17] reported that dendritic deformation could result in sliver grains

* Corresponding author.
E-mail address: linliu@nwpu.edu.cn (L. Liu).

http://dx.doi.org/10.1016/j.vacuum.2016.06.016

(one kind of SG in airfoil section) due to the asymmetrical contraction of the solidifying dendrites. Whether SG in the platform is originated from an independent heterogeneous nucleation process or from the deformation or fragmentation of the already-existed solidifying dendrites needs to be carefully studied.

The present study was dedicated to confirm the origin of SG through experimentally inspecting the macro-, microstructure and orientation distribution in SG sample in comparison with its' No-SG counterpart. On the basis of the conclusively determined origination of SG, micron-scale phenomenon was presented thereafter mainly focusing on the dimensions and morphologies of the γ' precipitation around the defect area. The solute segregation behavior around the area was also investigated to evaluate the harmful effect of SG formation from the perspective of the solute profile.

2. Experimental

2.1. Casting process

2.1.1. Blade geometry

A simplified model of a typical turbine blade consisting of a rectangle airfoil section and a foursquare platform as shown in Fig. 1(a) was used in present study to fabricate SXs using seeding-grain selection technique reported elsewhere in Ref. [18]. Seeds' orientations were precisely controlled as [100]//X, [010]//Y and [001]//Z according to the default coordinate system as illustrated in Fig. 1(b) and (c).

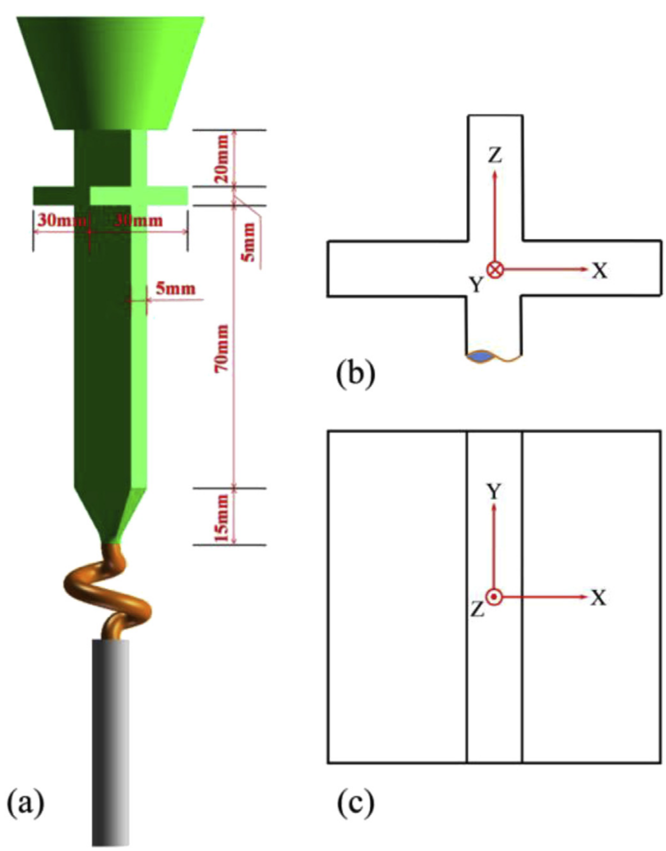

Fig. 1. Schematic of the simplified blade model assembly with a spiral grain selector (a) and the front-view (b) and the top-view (c) of the default coordinate system.

2.1.2. Molds and seeds preparation

Each part of the casting was prepared by injecting molten wax into corresponding mold and then assembled to an integrity. The assembly was then coated with ceramic slurry consisting of a binder and filler material (80% alumina and 20% silica) with additions of wetting and antifoaming agents to improve slurry rheology. The surface was stuccoed with coarse ceramic grit to adhere to the wet coating and harden it. To build up the shell thickness, six layers were successively built, including the primary coating, and 2-h intervals were used to dry every successive layer. After the shell was constructed, the molds were then dewaxed in a steam autoclave, and subsequently fired at 800 °C to partially sinter the ceramic shell. Seeds used in study were prefabricated using cylinder bars by traditional spiral grain selection technique. These SX bars were then cut into seeds' geometry with desired orientation. Seeds were then slotted into the mold whereafter from the bottom opening and adjusted until the expected arrangement of seeds to molds satisfied. The seeds were then fixed in mold.

2.1.3. Directional solidification process

The composition of alloys used in study is listed in Table 1. The SX castings were prepared using a modified Bridgman directional casting furnace (Fig. 2). During directional solidification, the furnace chamber was first evacuated to a partial pressure of approximately 10^{-2} Pa to prevent the melt being oxidized by using the combined pump system of a mechanical pump, a roots pump and a diffusion pump. The ceramic mold with seed was mounted and fastened on a water-cooled copper chill plate, and was then preheated to 1550 °C by graphite heating elements. After the ingot was melted, the liquid melt of 1500 °C was poured into the preheated mold cavity and held for 10 min to stabilize. Finally, the ceramic mold was withdrawn out of the furnace chamber at a predetermined rate of 6 mm min^{-1}.

2.2. Characterization procedure

After the casting process, the remnant mold was removed from blade surface with sandpaper. The platform areas were then sectioned transversely along the plane 0.5 mm above the platform base and prepared for macro defects inspection by submerging the samples into a solution of 50% HCl and 50% H_2O_2 for approximately 10 min. The macroetched samples were then metallographically prepared using a solution of 10 ml HNO_3: 20 mL HF: 30 mL $C_3H_8O_3$ for characterizing the dendritic morphologies. Average primary dendrite arm spacings (PDAS), λ_1, were calculated assuming a square array:

$$\lambda_1 = (A/n)^{0.5} \tag{1}$$

where n is the number of primary dendrite cores in the measured area A. All dendrites in the picked areas were included for calculation. γ' precipitation around GB area were observed in a scanning electron microscope (SEM, TESCAN). Electron Back-Scattering Diffraction (EBSD) mapping technique was employed to reveal the crystallographic orientation of the interest areas. Samples were cut and mechanically polished to remove stress and obtain a flat surface. EBSD measurements were performed in a scanning

Table 1
Nominal compositions of the alloys used in study (wt%).

Alloys	Cr	Co	Mo	W	Al	Ti	Ta	Re	Ni
A	9.5	5.0	3.8	5.2	5.9	2.1	–	–	Bal.
B	4.95	11.9	1.01	5.8	6.03	–	7.96	4.96	Bal.